New Journal of Physics
An Institute of Physics and Deutsche Physikalische Gesellschaft Journal

Electronic structure and the field emission mechanism of MgO-coated carbon nanotubes

Young-Woo Son[1], **Seungwu Han**[2,3] **and Jisoon Ihm**[1]
[1] School of Physics, Seoul National University, Seoul 151-742, Korea
[2] Princeton Materials Institute, Princeton University, Princeton, NJ 08544, USA
[3] Department of Physics, Ewha Womans University, Seoul 120-750, Korea
E-mail: jihm@snu.ac.kr

New Journal of Physics **5** (2003) 152.1–152.9 (http://www.njp.org/)
Received 4 August 2003
Published 14 November 2003

Abstract. In an attempt to improve the field emission (FE) characteristics of carbon nanotubes (CNTs), we have performed a first-principles study on MgO-coated CNTs. A MgO slab covering a CNT tip under a strong electric field shows dielectric screening behaviours with applied electric fields up to 0.3 V Å^{-1} and the effective dielectric constant approaches the bulk value within a few MgO layers. It is also found that the surface conduction band state of the MgO slab shifts down to the Fermi level as the applied electric field increases, indicating a FE mechanism different to that for CNTs without insulator coating. Electron emission via the surface conduction band of the insulator at the Fermi level is expected to enhance the FE current significantly, in agreement with a recent experiment.

Contents

PII: S1367-2630(03)67035-7

1. Introduction

Since the discovery of carbon nanotubes (CNTs) [1], there have been great efforts to study their novel physical properties as well as to pursue various applications taking advantage of these properties. For example, exploiting the unique electronic and mechanical characteristics of CNTs, successful fabrications of units of nanoscale logical circuits, biosensors and nanometre-size tweezers have been reported [2]–[4]. Among many promising applications of the CNT, the field emission (FE) electron source is believed to be a candidate for the most immediate realization [5]. Considering its exceptionally high aspect ratio, good conduction and low threshold voltage, the CNT has been regarded as an ideal field emitter for use in field emission displays (FEDs), cold cathode components in microwave power amplifiers, and miniature x-ray sources [6]–[8].

The requirement of long-time stability of the FE current under moderate vacuum conditions, a prerequisite for the application of FE sources, is, however, not easily fulfilled even though the durability of CNT FE tips is far better than that of conventional micron-sized metal tips. One of the most serious problems of the conventional microtip is substantial degradation in the emission current during exposure to oxygen molecules or water [9]. Moreover, ion bombardment under an extremely high local field can destroy or change the morphology of the microtip. A similar problem, although less severe than for the micron-sized tip, arises in nanotube FE tips. To overcome such drawbacks, boron nitride coating on CNT FE tips has been considered [10] on the same basis as coating micron-sized metal tips with semiconductors [11, 12]. Moreover, in the extremely strong electric field of the FED, the hybrid system composed of the metallic CNT and the insulating hard material is expected to exhibit unusual electronic characteristics which may be useful for applications.

Among various candidates for use as the coating material, the MgO multilayer has been chosen here because of its superior chemical inertness, mechanical hardness and small positive electron affinity (∼0.85 eV). On the experimental side, it was recently reported [13] that coating with a wide-bandgap material such as MgO or SiO_2 gives excellent emission characteristics and that the current stability is improved during exposure to oxygen molecules which are regarded as a critical current degradation source [14]. To understand the electronic structure and the FE mechanism of the insulator coating on the CNT, we have performed *ab initio* pseudopotential calculations for MgO-coated (two to seven monolayers) (5, 5) single-wall nanotubes (SWNTs) with variable magnitude of the applied electric field (0.0–0.3 V $Å^{-1}$).

The rest of the paper is organized as follows. The calculational method and the model system are described in section 2. Detailed results of the calculation are presented in section 3 and the conclusions in the last section.

2. Calculational method and model systems

Numerical calculations based on the first-principles pseudopotential method are carried out to obtain the ground state electronic structure. The local density approximation (LDA) is employed in setting up the exchange–correlation potential [15]. Troullier–Martins-type pseudopotentials [16] are used and the nonlocal part is converted into Kleinman and Bylander's fully separable form [17]. We perform the *ab initio* calculation with a plane wave basis to obtain the relaxed geometries for the CNT and MgO slab separately, and put the two components together with a fixed distance between them. Then we replace the plane wave basis with atomic-

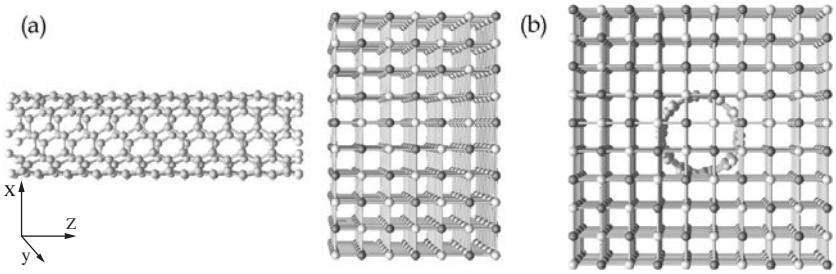

Figure 1. (a) A side view and (b) a top view of the ball and stick model for the seven-layer MgO(001) coating of the (5, 5) SWNT. Dangling bonds on each side of the CNT are passivated by hydrogen atoms. The black spots in the MgO layer are Mg atoms and the empty circles O atoms.

orbital-like basis functions following the method of Sankey and Niklewski [18]. Such localized basis functions make it possible to construct a realistic model with a large number of atoms in the unit supercell for our given computational capacity. Electronic structures of the system under an electric field of variable strength are obtained using a periodic saw-tooth-type potential for imitating the applied electric field in the supercell configuration. Therefore, our method produces self-consistent potentials and charge redistribution under the strong electric field beyond the linear response theory.

In the case of micron-long CNT tips, millions of atoms are involved and a realistic *ab initio* calculation is not feasible. However, it was previously found that the situation of the local electric field at the tip of a long CNT is well simulated by applying a higher electric field on a shorter tube [19]. We construct model systems which consist of a (5, 5) SWNT 24 Å in length and a flat MgO(001) multilayer on top of the SWNT. In figure 1, the ball and stick model of the system used for calculations is shown. The z-axis is parallel to the tube axis. The dangling bonds of the (5, 5) SWNT are passivated by hydrogen atoms and the distance between the seven-layer MgO(001) slab and the SWNT is set to 3 Å. The supercell size in the lateral (xy) direction is set at ∼20 Å to avoid interaction between (5, 5) SWNTs and that in the axial direction is set at ∼60 Å to allow sufficient vacuum regions. To study the effect of the thickness of the MgO(001) slab, we have also tested structures with different numbers of MgO monolayers.

3. Results

The size of the calculated energy gap of bulk MgO is found to be 4.42 eV which is quite a bit smaller than the experimental value of 7.83 eV. The LDA is known to underestimate the absolute gap value in general [20]. The smaller calculated gap would give rise to a larger dielectric constant. On the other hand, the present pseudopotential method ignores the core polarization which constitutes slightly more than half the total polarizability of MgO according to the literature [21]. The two effects happen to cancel each other roughly, but these two shortcomings of the LDA pseudopotential calculations for the dielectric screening can be serious limitations of the method and should be taken into account when necessary. The calculated bulk lattice constant of 4.22 Å and the small rumpling (<2.0%) at the MgO(001) surface agree well with the experiment and previous results [22, 23].

Using the self-consistent local potential, we can calculate the induced potential difference, $\delta V(\vec{r}) = V_{\text{local}}(\vec{r}; E_{\text{appl}} \neq 0) - V_{\text{local}}(\vec{r}; E_{\text{appl}} = 0)$. The contour plot on the plane crossing the

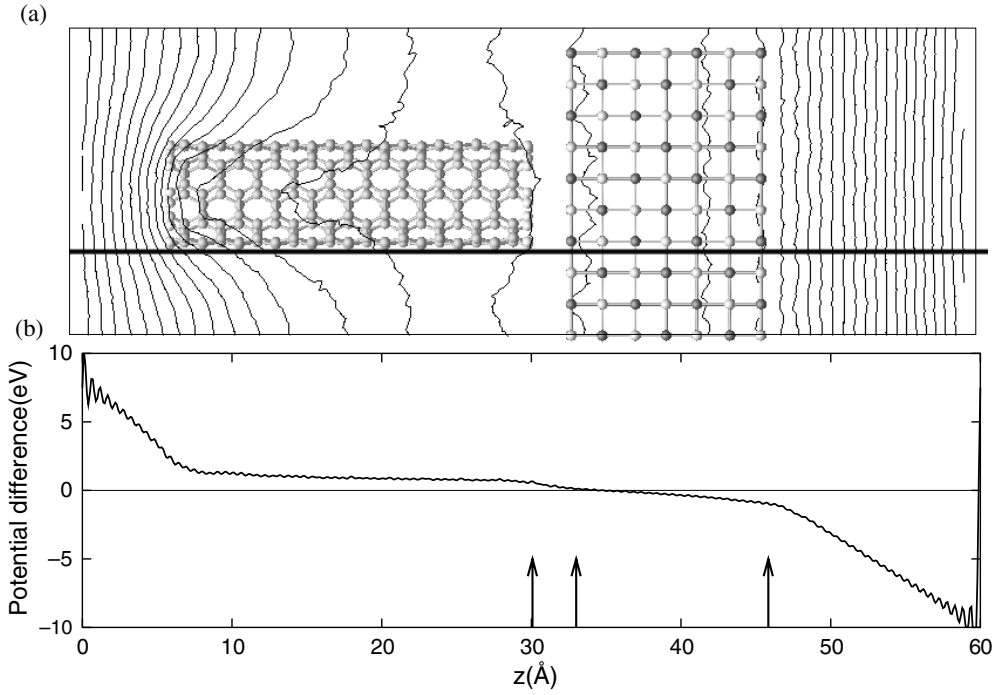

Figure 2. (a) The induced potential contour with the applied electric field $E_{\text{appl}} = 0.3$ V Å^{-1}. The contour interval is 0.05 V. (b) The line profile of the induced potential along the thick horizontal line in part (a). Three arrows, from left to right, indicate the positions of the end of the CNT, and the first and the seventh layers of MgO, respectively.

centre of the CNT is shown in figure 2(a). It is clearly illustrated that the (5, 5) CNT exhibits metallic screening (due to the small size of the model, there is a tiny but nonzero potential drop along the CNT) and, moreover, the seven-layer MgO slab shows dielectric screening behaviours. Noting that there is no large variation in the xy direction, the three-dimensional potential distribution can be approximated as a one-dimensional potential profile. The line profile for the induced potential along the thick line in figure 2(a) is shown in figure 2(b).

Because of the periodic boundary condition of the electrostatic potential (the fixed potential drop of the sawtooth potential across the supercell) and the screening by the CNT and MgO, the effective applied electric field experienced by the system, E_{eff}, can be shown to be

$$E_{\text{eff}} = E_{\text{appl}} \Big/ \left[1 - \frac{d_{\text{CNT}} + \frac{\epsilon-1}{\epsilon} d_{\text{MgO}}}{d_{\text{supercell}}}\right], \tag{1}$$

where d_{CNT} is the length of the (5, 5) CNT, d_{MgO} the thickness of the MgO slab, $d_{\text{supercell}}$ the length of the supercell in the z-direction, E_{appl} the nominal applied field chosen in the calculation (=total potential drop/$d_{\text{supercell}}$), and ϵ the static dielectric constant of the MgO slab (=9.65). In figure 3, the line profiles of the induced potentials with the nominal applied electric field of 0.3 V Å^{-1} are shown for models having different numbers of MgO layers. For comparison, the potentials for the (5, 5) CNT without the MgO slab are shown as well. As expected from equation (1), increase of E_{eff} with respect to E_{appl} occurs and the amount of increase changes depending on the relative magnitude of d_{MgO} and $d_{\text{supercell}}$. This enhancement is purely a computational artifact

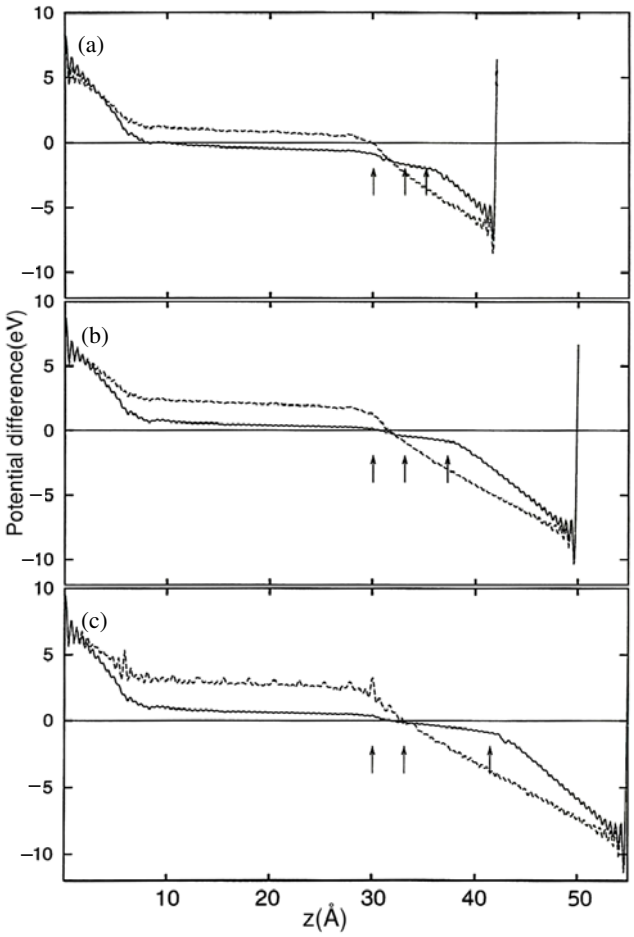

Figure 3. Induced potentials for various thicknesses of the MgO(001) slab under $E_{\text{appl}} = 0.3$ V Å^{-1} along the same line as in figure 2(a). Solid curves show the induced potentials for the MgO-coated CNTs and dotted curves those for the CNT without MgO layers. The arrows follow the same convention as in figure 2. The induced potential for the (5, 5) SWNT with two monolayers of MgO(001) is plotted in (a), that for three monolayers in (b), and that for five monolayers in (c).

to be taken into account in the calculation; it should be distinguished from the geometrical field enhancement factor at a sharp metallic edge. In fact, dielectric screening and the increased radius of curvature of the MgO-covered nanotube tip reduce the local field enhancement factor at the tip as compared to that for the bare CNT.

To find the induced charge under the applied electric field, we take the difference between the charge densities with and without an electric field along the z-direction, i.e., $\Delta\rho(z; E_{\text{appl}}) = \int[\rho(x, y, z; E_{\text{appl}} \neq 0) - \rho(x, y, z; E_{\text{appl}} = 0)]\,\mathrm{d}x\,\mathrm{d}y$. The resulting charge redistribution with $E_{\text{appl}} = 0.3$ V Å^{-1} is shown in figure 4(a). The accumulated charge at the outermost surface of the MgO(001) slab is found to be $-1.34|e|$. $\Delta\rho \simeq 0$ inside the tube region implies almost perfect screening of the metallic (5, 5) SWNT. The colour coded contour for the two-dimensional distribution of the induced charge on the plane passing through the centre of the CNT is shown in figure 4(b). The contour in figure 4(b) indicates that the induced charge at the surface of the

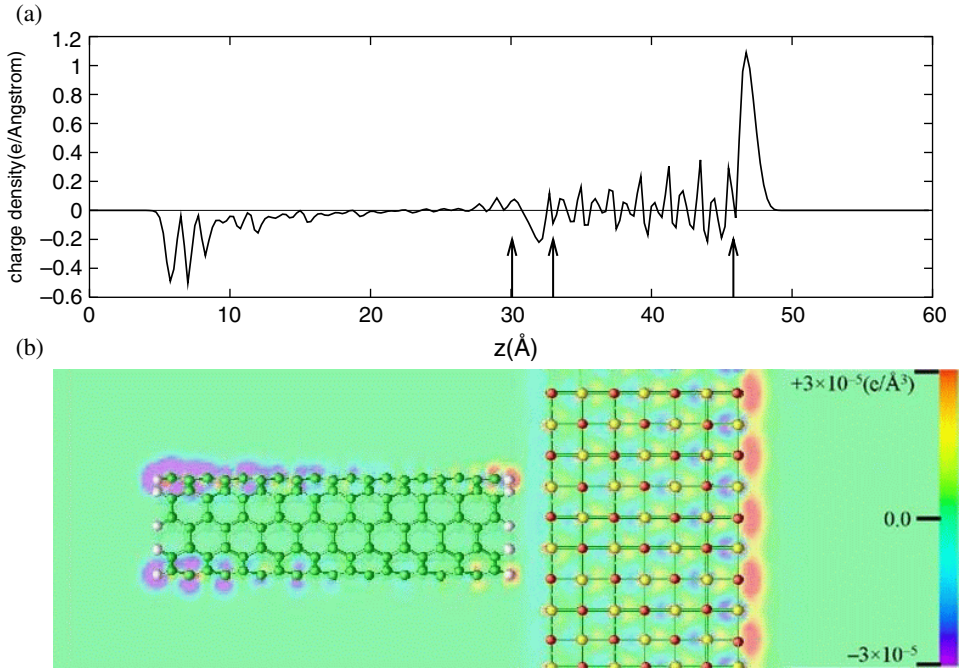

Figure 4. (a) The induced charge density along the axis of the CNT with $E_{\text{appl}} = 0.3$ V Å^{-1}. The arrows follow the same convention as in figure 2. (b) The colour indexing for the induced charge density on the plane cutting through the centre of the CNT.

MgO(001) slab is mostly located on Mg atoms and the charge around O atoms nearby at the surface is depleted.

To study the charge redistribution and the response of the wavefunction to the applied electric field, we plotted the projected density of states (PDOS) for each constituent species with and without an applied field, as shown in figure 5(a). The states around the Fermi level without an applied field originate from the (5, 5) SWNT and the energy levels of these states do not change much with applied electric fields up to 0.3 V Å^{-1}. In contrast, states originating from the MgO(001) slab, which are indicated by arrows (i)–(iv), show a sensitive response to the applied electric field. The state denoted by arrow (iii) resides at the Fermi level with $E_{\text{appl}} = 0.3$ V Å^{-1}. This large shift of the states with the applied electric field is presumably a characteristic of the localized state. Cross sectional views of the norms of the wavefunctions, $\rho_E(\vec{r}) = |\psi_E(\vec{r})|^2$, corresponding to states (i)–(iv) are presented in figure 5(b). The greyscale runs from white at zero density to black at the density of 1.0×10^{-5} e Å^{-3}. State (i), corresponding to the conduction band of the MgO slab, shows that most of the weight of the wavefunction is on the surface near the nanotube (innermost layer) while state (ii) shows that Mg atoms at the surface facing the vacuum region (outermost layer) have more weight than those at the innermost layer, and the coupling between the (5, 5) CNT and the MgO slab induces the state at the nearest layer of the MgO slab to the CNT. The situation changes dramatically when an electric field is applied. $\rho_E(\vec{r})$ corresponding to state (iii) at the Fermi level with $E_{\text{appl}} = 0.3$ V Å^{-1} is shown in figure 5(b)(iii). In this occupied state, the largest weight is on the outermost layer of the MgO slab which produced the dielectric screening. On the other hand, the still unoccupied state (iv) shows the largest weight on the surface adjacent to the CNT.

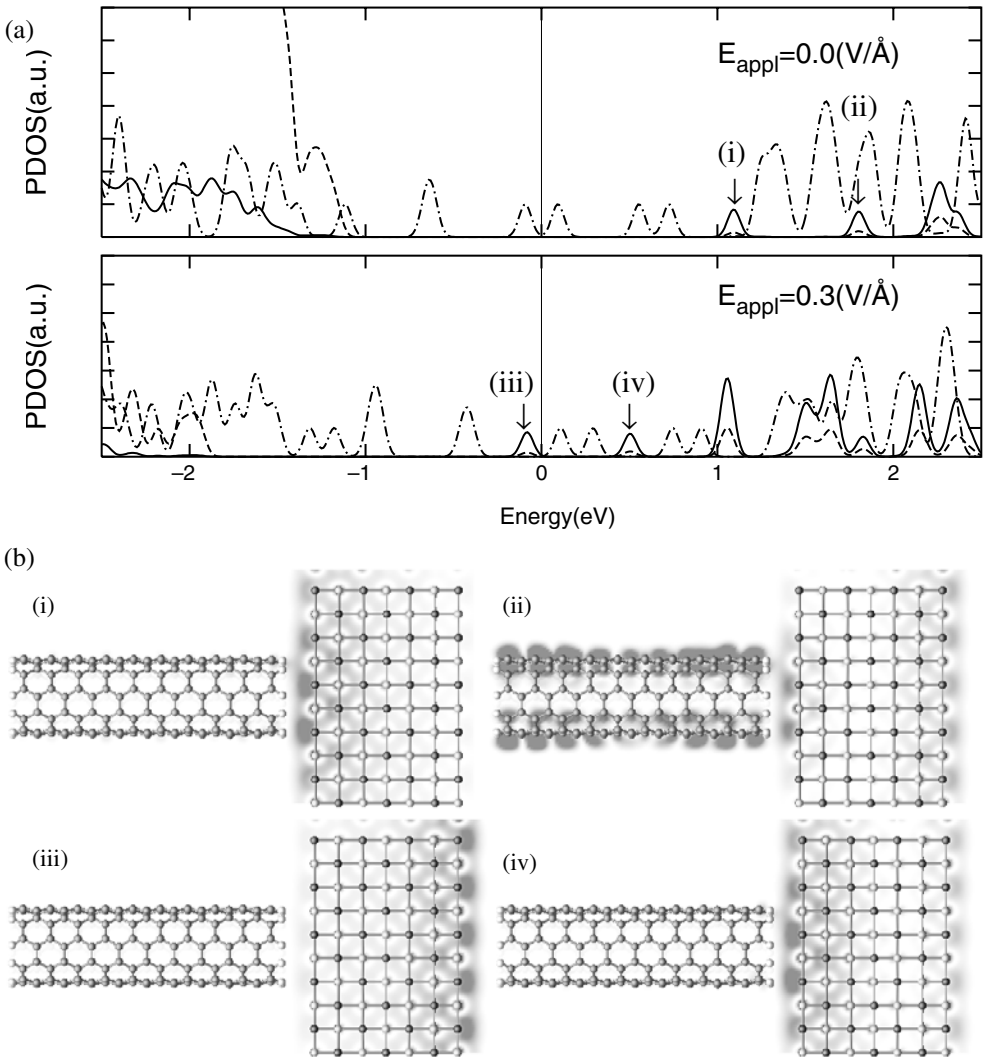

Figure 5. (a) The PDOS for the seven-layer MgO-coated (5, 5) CNT without an applied field and with $E_{\text{appl}} = 0.3$ V Å^{-1}. The Fermi level is set to zero. The dash–dotted curve shows the DOS of the (5, 5) CNT with hydrogen passivation. The dotted curve and the solid curve indicate the projected DOSs for the oxygen and magnesium atoms in the MgO slab, respectively. (b) The spatial distributions of the norm of the wavefunctions indicated by arrows (i)–(iv) in (a).

The energy positions of states (i)–(iv) change systematically as the applied electric field increases from 0.0 to 0.3 V Å^{-1} as shown in the DOS plot in figure 6. The states corresponding to the conduction band and the one above it show a rapid downward shift (∼0.3 eV) to the Fermi level with the small applied field of 0.03 V Å^{-1}. These states move down to the Fermi level by a further similar amount with a larger electric field of 0.1 V Å^{-1} (figure 6(c)). Finally, with $E_{\text{appl}} = 0.3$ V Å^{-1}, the conduction band of the Mg(001) slab shifts down to the Fermi level. This implies that the electrons emitted from the CNT pass through the conduction band of the coating insulator. Considering the PDOSs of figures 5 and 6, one sees that the emission mechanism

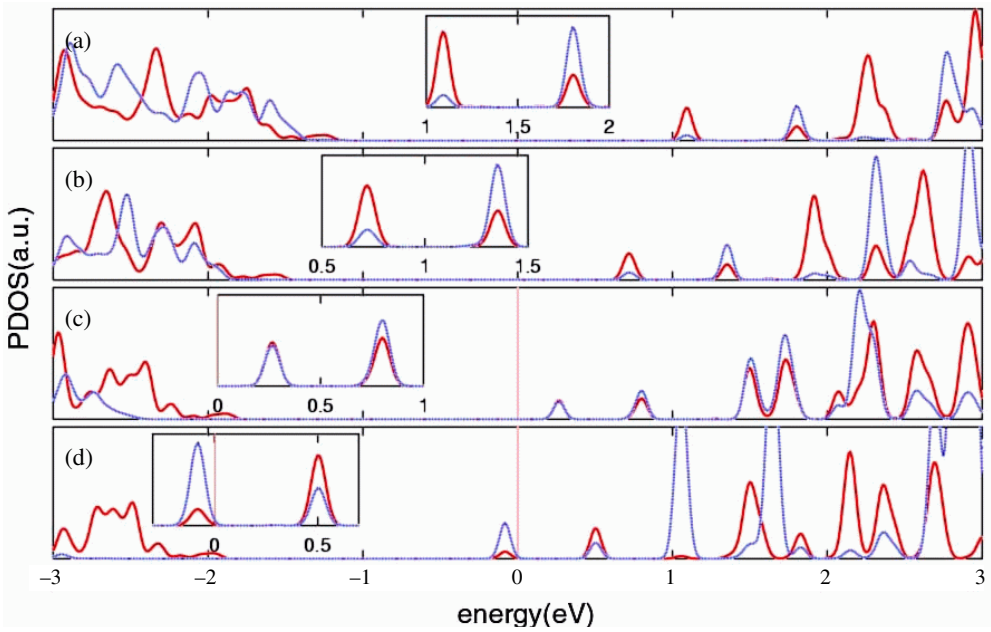

Figure 6. The PDOSs for the Mg atoms in the two outermost layers of the seven-layer MgO-coated (5, 5) CNT (a) without an applied electric field, (b) with an applied electric field of 0.03 V Å^{-1}, (c) with an applied electric field of 0.1 V Å^{-1}, and (d) with an applied electric field of 0.3 V Å^{-1}. The red curve is the DOS for Mg atoms in the layer adjacent to the CNT and the blue curve that for Mg atoms in the layer adjacent to the vacuum. The Fermi level is set to zero. The insets are enlarged views of the PDOSs at the energy levels denoted on the abscissas.

of the MgO-coated (5, 5) SWNT is different from that of the uncoated (5, 5) SWNT in which the localized state at the tip end dominates the emission current [19]. Since the major emission state is the surface conduction band state of the MgO slab, we expect the peak of the energy distribution curve for the emitted electrons to follow the shift in energy of the conduction band of MgO, in agreement with the experimental data in [13]. Moreover, the fact that the surface conduction band level lies, unlike the Fermi level of the CNT, very close to the vacuum level helps lower the onset voltage for the FE and increases the current. In practice, a certain minimum thickness ($\lesssim$100 Å) is necessary to achieve a smooth and well-ordered coating. However, for a much thicker ($>$100 Å) coating, the inevitable increase in the rate of scattering of electrons by the insulating material (i.e., by both the structural imperfections and phonons) will eventually overcome these merits and degrade the FE current.

4. Conclusions

Using the *ab initio* pseudopotential method, we have investigated the electronic structure and FE mechanism of MgO-coated CNTs under realistically strong electric fields. An ultrathin insulating MgO slab is capable of showing the bulk dielectric screening effect. Moreover, under a strong electric field, the surface conduction band state of the MgO slab is found to shift downward to the Fermi level. Under such circumstances, emitted electrons pass through the conduction

band of the MgO slab and reach the vacuum region, experiencing a low and narrow tunnelling barrier. Therefore, the insulating MgO layers not only protect the CNT tip from bombardment with accelerated ions but also enhance the emission current through an emission mechanism different to that in the bare CNT case. The emission characteristics expected from the present study are in good agreement with a recent experiment [13].

Acknowledgments

This work was supported by the CNNC of Sungkyunkwan University, the Samsung Advanced Institute of Technology, and the MOST through the National Science and Technology Programme (Grant No M1-0213-04-0001). The computation was done at the Supercomputing Centre of KISTI through the Grand Challenge Programme.

References

[1] Iijima S 1991 *Nature* **354** 56
[2] Dekker C 1999 *Phys. Today* **5** 22
[3] Chen R J *et al* 2003 *Proc. Natl Acad. Sci. USA* **100** 4984
[4] Kim P and Lieber C M 1999 *Science* **286** 2148
[5] Bonard J M, Kind H, Stöckli T and Nilsson L-O 2001 *Solid-State Electron.* **45** 893 and references therein
[6] Choi W B *et al* 1999 *Appl. Phys. Lett.* **75** 3129
Lee N S *et al* 2000 *Japan. J. Appl. Phys.* I **39** 7154
[7] Yue G Z *et al* 2002 *Appl. Phys. Lett.* **81** 355
[8] Bower C *et al* 2002 *Appl. Phys. Lett.* **80** 3820
[9] Chalamal B R, Wallace R M and Gnade B E 1998 *J. Vac. Sci. Technol.* B **16** 2859
Chalamal B R, Wallace R M and Gnade B E 1998 *J. Vac. Sci. Technol.* B **17** 303
[10] Park N, Han S and Ihm J 2003 *J. Nanosci. Nanotech.* **3** 179
[11] Shaw J L *et al* 1996 *J. Vac. Sci. Technol.* B **14** 2072
[12] Binh V T and Adessi Ch 2000 *Phys. Rev. Lett.* **85** 864
[13] Yi W *et al* 2002 *Adv. Mater.* **14** 1464
[14] Dean K A and Chalamala B R 1999 *Appl. Phys. Lett.* **75** 3017
Wadhawan A, Stallcup R E II and Perez J M 2001 *Appl. Phys. Lett.* **78** 108
[15] Ceperley D M and Alder B J 1980 *Phys. Rev. Lett.* **45** 566
[16] Troullier N and Martins J L 1991 *Phys. Rev.* B **43** 1993
[17] Kleinman L and Bylander D M 1982 *Phys. Rev. Lett.* **48** 1425
[18] Sankey O F and Niklewski D J 1989 *Phys. Rev.* B **40** 3979
[19] Han S and Ihm J 2002 *Phys. Rev.* B **66** 241402(R)
[20] Jones R O and Gunnarsson O 1989 *Rev. Mod. Phys.* **61** 689
[21] Umari P and Pasquarello A 2002 *Phys. Rev. Lett.* **89** 157602
[22] Chang K J and Cohen M L 1984 *Phys. Rev.* B **30** 4774
[23] Li Y, Langreth D C and Pederson M R 1997 *Phys. Rev.* B **55** 16456